Steel and Composite Structures, Vol. 9, No. 5 (2009) 473-497
DOI: http://dx.doi.org/10.12989/scs.2009.9.5.473

Dynamic stiffness matrix of composite box beams

Nam-Il Kim

Department of Civil and Environmental Engineering, Myongji University, San 38-2, Nam-Dong, Yongin, Kyonggi-Do, 449-728, Korea

(Received January 19, 2009, Accepted September 16, 2009)

Abstract. For the spatially coupled free vibration analysis of composite box beams resting on elastic foundation under the axial force, the exact solutions are presented by using the power series method based on the homogeneous form of simultaneous ordinary differential equations. The general vibrational theory for the composite box beam with arbitrary lamination is developed by introducing Vlasov°Øs assumption. Next, the equations of motion and force-displacement relationships are derived from the energy principle and explicit expressions for displacement parameters are presented based on power series expansions of displacement components. Finally, the dynamic stiffness matrix is calculated using force-displacement relationships. In addition, the finite element model based on the classical Hermitian interpolation polynomial is presented. To show the performances of the proposed dynamic stiffness matrix of composite box beam, the numerical solutions are presented and compared with the finite element solutions using the Hermitian beam elements and the results from other researchers. Particularly, the effects of the fiber orientation, the axial force, the elastic foundation, and the boundary condition on the vibrational behavior of composite box beam are investigated parametrically. Also the emphasis is given in showing the phenomenon of vibration mode change.

Keywords : free vibration; composite box beam; dynamic stiffness matrix; foundation effect.

1. Introduction

Advanced composite materials have been increasingly used over the past few decades as their high ratio of stiffness and strength to weight. Other advantages that motivate some applications are corrosion resistance, magnetic transparency, low thermal expansion, and excellent fatigue characteristics in the direction of the fibers. Recently, Walker (2007) described a methodology to design symmetrically laminated fiber-reinforced structures under transverse loads for minimum weight, with manufacturing uncertainty in the ply angle. For any structure that may be subjected to dynamic loads, the determination of the natural frequencies and its mode shapes is critical in the design process. It is usually the first step in a dynamic analysis since a great deal may be deduced concerning the structural behavior and integrity from the knowledge of its natural frequencies and mode shapes.

Up to the present, considerable research efforts to obtain analytical solutions for the vibration analysis of composite beams have been made by many researchers. Matsunaga (2001) derived a set of fundamental dynamic equations of one-dimensional higher-order theory for laminated composite beams through Hamilton's principle by using the method of power series expansion of displacement components. Qin

Research Professor, Email: kni8501@gmail.com

and Librescu (2002) investigated the non-classical effects on the natural frequencies using the extended Galerkin's method within the framework of an existing anisotropic thin-walled beam model. Song and Librescu (1997) performed an analytical study devoted to the mathematical modeling of spinning anisotropic thin-walled beams. Also Song and Librescu (1993) presented the formulation of the dynamic problem of laminated composite thick- and thin-walled, single-cell beams of arbitrary cross-section. The structural model considered the exotic properties characterizing the advanced composite material structures such as the anisotropy and the heterogeneity. The free vibration solution of stepped laminated composite beams of rectangular cross-section using a simple higher- order theory which assumes a cubic distribution for the displacement field through the thickness was studied by Song and Waas (1997). They used a method of separation of variables to governing equations and obtained 12 homogenous linear algebraic equations by applying appropriate boundary conditions. Armanios and Badir (1995) investigated the dynamic response of thin-walled box composite beams using the asymptotic variational approach. The analysis is applied for two lay-up configurations, namely the circumferentially uniform stiffness (CUS) and the circumferentially antisymmetric stiffness (CAS). Dancila and Armanios (1998) used the governing equations provided by Armanios and Badir (1995) to develop a simple quasi-decoupled solution procedure that provides accurate predictions of natural frequencies with little computational effort.

As an alternative approach, the transfer matrix method has been used to calculate the natural frequency of composite beam. Yildirim, *et al*. (1999) studied in-plane and out-of-plane free vibration problems of symmetric cross-ply laminated composite beams using the transfer matrix method. As a continuation of Yildirim, *et al*. (1999), Yildirim and Kiral (2000) performed the out-of-plane bending and torsional free vibration analysis of symmetric cross-ply laminated composite beams. The relative difference between the first six non-dimensional frequencies obtained by the Bernoulli-Euler and Timoshenko beam theories was presented for different length to thickness ratios, thickness to width ratios, and different types of boundary conditions.

On the other hand, the finite element method has been widely used because of its versatility and a large amount of work was devoted to the improvement of composite finite elements in order to obtain the acceptable results. La, *et al*. (2007) investigated the effects of randomness in material properties and foundation stiffness parameters on the free vibration response of laminated composite plate resting on an elastic foundation using a C^o finite element method. Kisa and Gurel (2005) studied the modal analysis of cracked cantilever composite beams, made of graphite-fibre reinforced polyamide using the finite element and component mode synthesis method. Lee and Kim (2000, 2002) developed a displacement based one-dimensional finite element model to predict natural frequencies and corresponding vibration modes for a thin-walled composite I- and channel-beams. The displacements expressed over each element as a linear combination of the one-dimensional Lagrange interpolation function and Hermite-cubic interpolation function. Through numerical results, they addressed the effects of fiber angle, modulus ratio, height-to-thickness ratio, and boundary conditions on the vibration frequencies of composite beam. Thereafter, Vo and Lee (2008) studied the free vibration analysis of a thin-walled laminated composite beam with box section using the finite element developed by Lee and Kim (2000, 2002). Shi and Lam (1999) presented the derivation of the variational consistent stiffness and mass matrices for the finite element modeling of a composite beam. The two-noded higher-order composite beam element possessed a linear bending strain as opposed to the constant bending strain in the existing higher-order composite beam elements with the same number of nodal degrees of freedom. The free vibration characteristics of laminated composite beams using the finite element analysis and the higher-order plate theory were studied by Chandrashekhara and Bangera (1992). They incorporated a Poisson effect, which was often neglected in one-dimensional laminated beam analysis, in the formulation of the beam

constitutive equation. Marur and Kant (1996) proposed three higher-order displacement models for free vibration analysis of composite beams with various boundary conditions and aspect ratios using the finite element modeling based on isoparametric formulations and Wu and Sun (1990) developed a two-noded, 10 degrees of freedom per node, laminated composite thin-walled beam finite element for vibration analysis based on modified assumptions of classical isotropic thin-walled beam theory. Also Ashour (2003) employed a finite strip transition matrix technique to obtain the natural frequencies of symmetric cross-ply laminated composite plates with edges elastically restrained against both translation and rotaion.

The exact element method based on the solutions of the ordinary differential equations was used as an effective method solving the dynamic problem of isotropic and composite beams. The method of solution by power series that yields the exact dynamic stiffness matrix was first introduced by Eisenberger (1990). Since then it was used by the same author for many problems of beams including the higher order models (Eisenberger 2003a, 2003b) and the torsional vibration of open and variable cross-sections (Eisenberger 1995, 1997). Also Eisenberger (1994) evaluated the exact vibration frequencies of beam resting on variable one- and two-parameter elastic foundation using the dynamic stiffness matrix of beam. Eisenberger and Abramovich (1997), Eisenberger, *et al*. (1995), and Abramovich, *et al*. (1995, 1996) applied the exact element method presented by Eisenberger (1990) to calculate the natural frequencies and the mode shapes of laminated composite beams. Banerjee and Williams (1995, 1996) have developed the dynamic stiffness matrices of a composite beam in order to investigate their free vibration characteristics. The associated theories accounted for the effect of the material coupling between the bending and torsional modes of deformation which is usually present in composite beams, such as aircraft wings. And an explicit analytical expression for each of elements of the dynamic stiffness was derived by rigorous use of the symbolic computing package. Thereafter, Banerjee (1998) extended the earlier theories of Banerjee and Williams (1995, 1996) by including the effect of an axial force. However, the above-mentioned works considered only the dynamic stiffness of composite beam with rectangular cross-section.

The existing literature reveals that, even though a significant amount of research has been conducted on development of the free vibration analysis of thin-walled composite beam, there still has been no study of the exact dynamic stiffness of a composite box beams with arbitrary lamination in the literature. Also investigation into the influence of the axial force, the foundation, and the boundary condition on the coupled or decoupled vibrational behavior of composite box beam, and the vibration mode change phenomenon do not appear to have been reported.

The purpose of this study is to present the dynamic stiffness matrix that can be used in performing the free vibration analysis of box beams made from fiber-reinforced laminates with symmetric and arbitrary laminations. The present approach advocates the use of direct evaluation schemes using symbolic manipulation, rather than using a discrete integration scheme or a method based on energy principles which may perform poorly for stiff systems.

2. Vibration theory of composite box beam

For the vibration analysis of thin-walled composite box beam, following assumptions are adopted.

1. The composite box beam is slender and prismatic.
2. The Kirchhoff-Love assumption in classical theory is valid for thin-walled composite beams.
3. The cross-section is assumed to maintain its shape during deformation, so that there is no distortion.

4. Each laminate is thin and perfectly bonded.
5. The normal stress σ_s in the contour direction s is small compared to the axial stress σ_x.

For the theoretical developments presented in this study, the geometry and three sets of coordinate systems which are mutually interrelated are presented in Figs. 1 and 2, respectively. The first coordinate system is the orthogonal Cartesian coordinate system (x_1, x_2, x_3) and the second coordinate system is the local plate coordinate ($\bar{n}$, s, x_1) wherein the $\bar{n}$ axis is normal to the middle surface of a plate element, the s axis is tangent to the middle surface and is directed along the contour line of the cross-section. The third one is the contour coordinate S along the profile of the section with its origin at any point O on the profile section. The point P is called the pole axis.

The mid-plane displacement components u, v, and w of an arbitrary point in the contour coordinate system can be expressed according to the assumption 3 as follows:

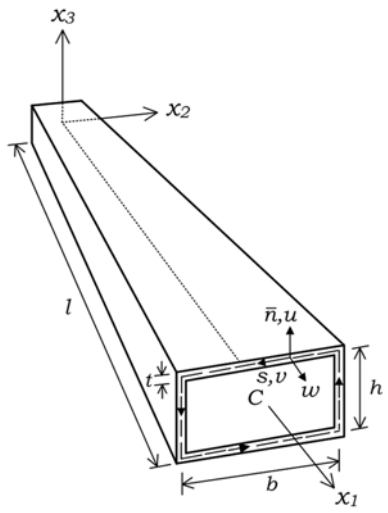

Fig. 1 Geometry and coordinate system of a composite box beam

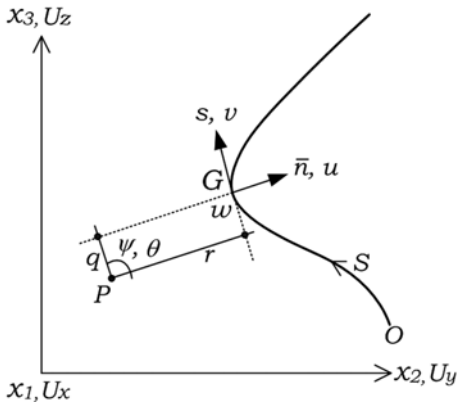

Fig. 2 Pictorial definitions of coordinates in thin-walled section

$$u(s,x_1) = U_y(x_1)\sin\psi(s) - U_z(x_1)\cos\psi(s) - \theta(x_1)q(s) \tag{1a}$$

$$v(s,x_1) = U_y(x_1)\cos\psi(s) + U_z(x_1)\sin\psi(s) + \theta(x_1)r(s) \tag{1b}$$

$$w(s,x_1) = U_x(x_1) - U'_y(x_1)x_2 - U'_z(x_1)x_3 - \theta'(x_1)\phi \tag{1c}$$

where U_x, U_y, and U_z are the rigid body translations with respect to x_1, x_2, and x_3 axes, respectively, and θ is the twisting angle. The angle ψ defines the relative orientation of the (x_1, x_2, x_3) and ($\bar{n}$, s, x_1) coordinate systems, and is equal to the angle between x_2 and s direction at G. The prime denotes the differentiation with respect to x_1 and ϕ is the normalized warping function at the pole point and given by

$$\phi(s) = \int_{c(s)} \left[r(s) - \frac{F_s(s)}{t(s)} \right] ds \tag{2}$$

where $F_s(s)$ and $t(s)$ are the St. Venant shear flow and the wall thickness, respectively; $c(s)$ is the segment of the contour lying between the origin and the arbitrary point. The general constitutive relations between the membrane forces and the bending and torsional moments and their strains and curvatures for the arbitrary laminate are as follows:

$$\begin{Bmatrix} \{N\} \\ \{M\} \end{Bmatrix} = \begin{bmatrix} [A] & [B] \\ [B] & [D] \end{bmatrix} \begin{Bmatrix} \{\varepsilon\} \\ \{\kappa\} \end{Bmatrix} \tag{3}$$

where the laminate resultant forces and moments are

$$\{N\} = \begin{Bmatrix} N_x \\ N_s \\ N_{xs} \end{Bmatrix}, \qquad \{M\} = \begin{Bmatrix} M_x \\ M_s \\ M_{xs} \end{Bmatrix} \tag{4a,b}$$

and the laminate strains and curvatures are

$$\{\varepsilon\} = \begin{Bmatrix} \varepsilon_x \\ \varepsilon_s \\ \gamma_{xs} \end{Bmatrix}, \qquad \{\kappa\} = \begin{Bmatrix} \kappa_x \\ \kappa_s \\ \kappa_{xs} \end{Bmatrix} \tag{5a,b}$$

In Eq. (3), the expressions for the stiffness submatrices [A], [B], and [D] are defined by Jones (1975). And ε_x and γ_{xs} indicate the axial and shear strains, respectively, and κ_x and κ_{xs} are the axial and twist curvatures, respectively, of the middle surface and are expressed as follows:

$$\varepsilon_x = \frac{\partial w}{\partial x_1} = U_x' - U_y'' x_2 - U''_z x_3 - \theta'' \phi \tag{6a}$$

$$\gamma_{xs} = \frac{\partial w}{\partial s} + \frac{\partial v}{\partial x_1} = \theta' \frac{F_s(s)}{t(s)} \tag{6b}$$

$$\kappa_x = \frac{\partial^2 u}{\partial x_1^2} = U_y'' \sin\psi - U_z'' \cos\psi - \theta'' q \tag{6c}$$

$$\kappa_{xs} = 2\frac{\partial^2 u}{\partial x_1 \partial s} = -2\theta' \tag{6d}$$

The appropriate assumptions for constitutive relations are essential for a refined composite beam theory since the pile in the laminated composites behave in a highly two-dimensional manner due to the Poisson's effect (Smith and Chopra 1991). In this regard, the zero hoop stress assumption is employed in this study. Assuming zero hoop stress leads to $N_s = M_s = 0$, and then the hoop strain, ε_s and the tangential curvature, κ_s can be expressed from Eq. (3) as follows:

$$\begin{aligned}\varepsilon_s = -\frac{1}{A_{22}D_{22} - B_{22}^2}\{&(A_{12}D_{22} - B_{12}B_{22})\varepsilon_x + (A_{26}D_{22} - B_{22}B_{26})\gamma_{xs} \\ &+ (B_{12}D_{22} - B_{22}D_{12})\kappa_x + (B_{26}D_{22} - B_{22}D_{26})\kappa_{xs}\}\end{aligned} \tag{7a}$$

$$\begin{aligned}\kappa_s = \frac{1}{A_{22}D_{22} - B_{22}^2}\{&(A_{12}D_{22} - A_{22}B_{12})\varepsilon_x + (A_{26}B_{22} - A_{22}B_{26})\gamma_{xs} \\ &+ (B_{12}B_{22} - A_{22}D_{12})\kappa_x + (B_{22}B_{26} - A_{22}D_{26})\kappa_{xs}\}\end{aligned} \tag{7a}$$

Substituting Eqs. (7a) and (7b) into Eq. (3) gives the reduced constitutive relation as follows:

$$\begin{Bmatrix} N_x \\ N_{xs} \\ M_x \\ M_{xs} \end{Bmatrix} = \begin{bmatrix} A_{11}^* & A_{16}^* & B_{11}^* & B_{16}^* \\ A_{16}^* & A_{66}^* & \tilde{B}_{16}^* & B_{66}^* \\ B_{11}^* & \tilde{B}_{16}^* & D_{11}^* & D_{16}^* \\ B_{16}^* & B_{66}^* & D_{16}^* & D_{66}^* \end{bmatrix} \begin{Bmatrix} \varepsilon_x \\ \gamma_{xs} \\ \kappa_x \\ \kappa_{xs} \end{Bmatrix} \tag{8}$$

Recently, for the static analysis of thin-walled composite beam with open-section, Shin, *et al*. (2007) derived the elastic strain energy, by using the transformation relationships developed by Gjelsvik

(1981) between the beam stress resultants and the plate ones, and the constitutive relations between the beam stress resultants and the displacements, as follows:

$$\Pi_E = \frac{1}{2}\int_o^l [A U'^2_x + I_3 U''^2_y + I_2 U''^2_z + 2I_{23} U''_y U''_z + I_\phi \theta''^2 + 2I_{\phi 3} U''_y \theta'' + 2I_{\phi 2} U''_z \theta'' + JG\theta'^2 - 2S_2 U'_x U''_z - 2S_3 U'_x U''_y - 2S_w U'_x \theta'' + 2S_\phi U'_x \theta' - 2H_s U''_y \theta' + 2H_c U''_z \theta' + 2H_q \theta' \theta'']dx_1 \tag{9}$$

where l denotes the length of beam and the detailed expressions of sectional quantities in Eq. (9) are presented in Appendix A. The potential energy Π_G due to the initial axial force ${}^oF_1$ can be represented as

$$\Pi_G = \frac{1}{2}\int_o^l [{}^oF_1(U'^2_y + U'^2_z) + {}^oF_1 R_p^2 \theta'^2]dx_1 \tag{10}$$

where R_p^2 denotes the geometrical characteristics considering the Wagner effect which reflects the effect of normal stress and section properties on the twisting behavior and is defined as (Bauld and Tzeng 1984)

$$R_p^2 = \frac{1}{A}\int_C A_{11}\left(r^2 + q^2 + \frac{D_{11}}{A_{11}}\right)ds \tag{11}$$

Also, the kinetic energy Π_M of the beam considering the rotary inertia effect is given by

$$\Pi_M = \frac{1}{2}\int_V \rho(\dot{u}^2 + \dot{v}^2 + \dot{w}^2)dV \tag{12}$$

where ρ is the density and substitution of displacement components into Eq. (12) leads to

$$\Pi_M = \frac{1}{2}\rho\omega^2 \int_o^l [A^*(U_x^2 + U_y^2 + U_z^2) + I_2^* U'^2_z + I_3^* U'^2_y + I_o^* \theta^2 + I_\phi^* \theta'^2 + 2A^*(y - y_p)U_z\theta - 2A^*(z - z_p)U_y\theta]dx_1 \tag{13}$$

where ω is the frequency of harmonic vibration; A^*, I_2^*, and I_3^* are the cross sectional area, the second moment of inertia about x_2 and x_3 axes, respectively; I_o^* and I_ϕ^* are the polar moment of inertia and the warping moment of inertia due to the normalized warping, respectively. These section properties are defined as follows:

$$A^* = \int_{A^*} dA^*, I_2^* = \int_{A^*} x_3^2 dA^*, I_3^* = \int_{A^*} x_2^2 dA^*, I_o^* = \int_{A^*} (q^2 + r^2)dA^*, I_\phi^* = \int_{A^*} \phi^2 dA^* \tag{14a-e}$$

In Eq. (13), the following geometric relations are used from Fig. 2.

$$y-y_p = q\cos\psi + r\sin\psi \tag{15a}$$

$$z-z_p = q\sin\psi - r\cos\psi \tag{15b}$$

Now, we consider the composite beam resting on elastic foundation as shown in Fig. 3, in which the k_x, k_y and k_z are the Winkler foundation moduli indicating the first type of foundation parameters for the axial and transverse translations at the point (h_y, h_z) and k_θ is the rotational parameter for rotation of the cross-section. And g_y and g_z denote the second type of foundation parameters i.e., Vlasov, Pasternak and Filonenko-Borodich foundation moduli at the point (h_y, h_z). Dube and Dumir (1996) presented the energy expression corresponding to the elastic foundation based on the classical beam theory for the free vibration analysis of isotropic thin-walled beam as follows:

$$\begin{aligned}\Pi_F = \frac{1}{2}\int_o^l [&k_x U_x^2 + k_y\{U_y-(h_z-z_p)\theta\}^2 + k_z\{U_z+(h_y-y_p)\theta\}^2 + k_\theta\theta^2 \\ &+ g_y\{U'_y-(h_z-z_p)\theta'\}^2 + g_z\{U'_z+(h_y-y_p)\theta'\}^2]dx_1\end{aligned} \tag{16}$$

Then, we consider the extended Hamilton's principle which can be expressed in the form

$$\int_{t_1}^{t_2}(\delta\Pi_E+\delta\Pi_G-\delta\Pi_M+\delta\Pi_F-\delta\Pi_{ext})dt = 0 \tag{17}$$

where Π_{ext} is the external work corresponding to the element nodal forces and δ is the variational operator.

Finally, substitution of Eqs. (9), (10), (13), and (16) into Eq. (17) and performing the variational operations give the following equations of motion and the force-displacement relationships as

$$AU_x''- S_3U_y''' - S_2U_z''' + S_\phi\theta'' - S_w\theta''' - k_xU_x + \rho\omega^2A^*U_x = 0 \tag{18a}$$

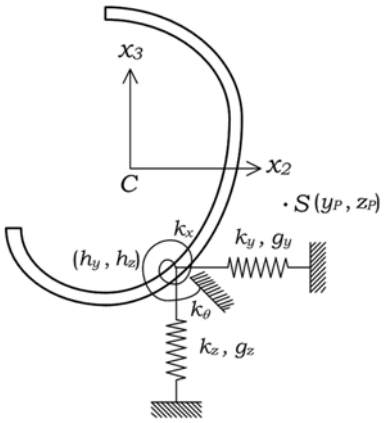

Fig. 3 Cross-section of beam on elastic foundation

$$\tilde{I}_3 U_y'''' + \tilde{I}_{23} U_z'''' - \tilde{H}_s \theta'''' + \tilde{I}_{\phi 3} \theta'''' - \frac{S_3 k_x}{A} U_x' - {}^{o}F_1 U_y'' + k_y \{ U_y - (h_z - z_p)\theta \}$$
$$- g_y \{ U_y'' - (h_z - z_p)\theta'' \} + \rho\omega^2 \left[\frac{A^*}{A} S_3 U_x' - A^* U_y + I_3^* U_y'' + A^* (z - z_p)\theta \right] = 0 \tag{18b}$$

$$\tilde{I}_{23} U_y'''' + \tilde{I}_2 U_z'''' + \tilde{H}_c \theta'''' + \tilde{I}_{\phi 2} \theta'''' - \frac{S_2 k_x}{A} U_x' - {}^{o}F_1 U_z'' + k_z \{ U_z + (h_y - y_p)\theta \}$$
$$- g_y \{ U_z'' + (h_y - y_p)\theta'' \} + \rho\omega^2 \left[\frac{A^*}{A} S_2 U_x' - A^* U_z + I_2^* U_z'' - A^* (y - y_p)\theta \right] = 0 \tag{18c}$$

$$- S_\phi U_x'' + H_s U_y'''' + \tilde{I}_{\phi 3} U_y'''' - H_c U_z'''' + \tilde{I}_{\phi 2} U_z'''' - JG\theta'' + \frac{S_\phi S_w}{A} \theta'''' + \tilde{I}_\phi \theta'''' - {}^{o}F_1 R_p^2 \theta'' - k_y (h_z - z_p) U_y$$
$$+ k_z (h_y - y_p) U_z + \{ k_y (h_z - z_p)^2 + k_z (h_y - y_p)^2 + k_\theta \} \theta + g_y (h_z - z_p) U_y'' - g_z (h_y - y_p) U_z'' - \{ g_y (h_z - z_p)^2$$
$$+ g_z (h_y - y_p)^2 \} \theta'' + \rho\omega^2 \left[\frac{A^*}{A} S_w U_x' + A^* (z - z_p) U_y - A^* (y - y_p) U_z - I_o^* \theta + I_\phi^* \theta'' \right] = 0 \tag{18d}$$

where

$$\tilde{I}_2 = I_2 - \frac{S_2^2}{A}, \quad \tilde{I}_3 = I_3 - \frac{S_3^2}{A}, \quad \tilde{I}_{23} = I_{23} - \frac{S_2 S_3}{A}, \quad \tilde{I}_\phi = I_\phi - \frac{S_w^2}{A}$$
$$\tilde{I}_{\phi 2} = I_{\phi 2} - \frac{S_2 S_w}{A}, \quad \tilde{I}_{\phi 3} = I_{\phi 3} - \frac{S_3 S_w}{A}, \quad \tilde{H}_s = H_s - \frac{S_3 S_\phi}{A}, \quad \tilde{H}_c = H_c + \frac{S_2 S_\phi}{A} \tag{19a-h}$$

and force-displacement relationships are as follows:

$$F_1 = A U_x' - S_3 U_y'' - S_2 U_z'' + S_\phi \theta' - S_w \theta'' \tag{20a}$$

$$F_2 = -\tilde{I}_3 U_y''' - \tilde{I}_{23} U_z''' + \tilde{H}_s \theta'' - \tilde{I}_{\phi 3} \theta''' + {}^{o}F_1 U_y' + g_y \{ U_y' - (h_z - z_p) \} \theta' - \rho\omega^2 \left(\frac{A^*}{A} S_3 U_x + I_3^* U_y' \right) \tag{20b}$$

$$F_3 = -\tilde{I}_{23} U_y''' - \tilde{I}_2 U_z''' - \tilde{H}_c \theta'' - \tilde{I}_{\phi 2} \theta''' + {}^{o}F_1 U_z' + g_z \{ U_z' + (h_y - y_p) \} \theta' - \rho\omega^2 \left(\frac{A^*}{A} S_2 U_x + I_2^* U_z' \right) \tag{20c}$$

$$M_1 = S_\phi U_x' - H_s U_y'' - \tilde{I}_{\phi 3} U_y''' + H_c U_z'' - \tilde{I}_{\phi 2} U_z''' + JG\theta' - \frac{S_\phi S_w}{A} \theta'' - \tilde{I}_\phi \theta''' + g_z (h_y - y_p) U_z'$$
$$- g_y (h_z - z_p) U_y' - g_y (h_z - z_p) U_y' + \{ {}^{o}F_1 R_p^2 + g_y (h_z - z_p)^2 + g_z (h_y - y_p)^2 \} \theta'$$
$$- \rho\omega^2 \left(\frac{A^*}{A} S_w U_x + I_\phi^* \theta' \right) \tag{20d}$$

$$M_2 = S_2 U_x' - I_{23} U_y'' - I_2 U_z'' - H_c \theta' - I_{\phi 2} \theta'' \tag{20e}$$

$$M_3 = -S_3 U_x' + I_3 U_y'' + I_{23} U_z'' - H_s \theta' + I_{\phi 3} \theta'' \tag{20f}$$

$$M_\phi = S_w U_x' - I_{\phi 3} U_y'' - I_{\phi 2} U_z'' - H_q \theta' - I_\phi \theta'' \tag{20g}$$

3. Evaluation of dynamic stiffness matrix of composite box beam

3.1 Evaluation of displacement function

For the dynamic stiffness matrix of composite box beam, it is necessary to evaluate the displacement function of beam. For this, we consider the following displacement state vector consisting of 14 displacement parameters defined by

$$\mathbf{d}(\mathbf{x}) = \langle U_x,\ U_x',\ U_y,\ U_y',\ U_y'',\ U_y''',\ U_z,\ U_z',\ U_z'',\ U_z''',\ \theta,\ \theta',\ \theta'',\ \theta''' \rangle^T \tag{21}$$

The solutions of four displacements are taken as the following infinite power series.

$$U_x = \sum_{n=0}^{\infty} a_n x^n, \quad U_y = \sum_{n=0}^{\infty} b_n x^n, \quad U_z = \sum_{n=0}^{\infty} c_n x^n, \quad \theta = \sum_{n=0}^{\infty} d_n x^n \tag{22a-d}$$

Next, substituting Eq. (22) into Eq. (18) and shifting the index of power of x^n, the equations of motion are expressed as power series expansions of displacement components and presented in Appendix B. Also these equations can be expressed compactly in a matrix form as follows:

$$\sum_{n=0}^{\infty} \mathbf{A_n} \{a_{n+2}, b_{n+4}, c_{n+4}, d_{n+4}\}^T$$

$$= \sum_{n=0}^{\infty} \mathbf{B_n} \{a_n, a_{n+1}, b_n, b_{n+1}, b_{n+2}, b_{n+3}, c_n, c_{n+1}, c_{n+2}, c_{n+3}, d_n, d_{n+1}, d_{n+2}, d_{n+3}\}^T \tag{23}$$

Then, we consider the initial integration constant vector **a** as follows:

$$\mathbf{a} = \{a_0, a_1, b_0, b_1, b_2, b_3, c_0, c_1, c_2, c_3, d_0, d_1, d_2, d_3\}^T \tag{24}$$

From Eq. (23), the following relation is obtained.

$$\{a_{i+2}, b_{i+4}, c_{i+4}, d_{i+4}\}^T = \mathbf{Z_i} \{a_i, a_{i+1}, b_i, b_{i+1}, b_{i+2}, b_{i+3}, c_i, c_{i+1}, c_{i+2}, c_{i+3}, d_i, d_{i+1}, d_{i+2}, d_{i+3}\} = \mathbf{Z_i N_i a} \tag{25}$$

where

$$\mathbf{Z_i} = \mathbf{A_i^{-1}B_i} \tag{26}$$

In Eq. (25), the terms for $a_{i+2}, b_{i+4}, c_{i+4},$ and d_{i+4} and converge to zero as $i \to \infty$. The displacement state vector in Eq. (21) is expressed with respect to the initial integration constant vector **a** by using Eqs. (22) and (25) as follows:

$$\mathbf{d} = \mathbf{X_n a} \tag{27}$$

where $\mathbf{X_n}$ denotes the 14 × 14 matrix function with the coefficients of U_x, U_y, U_z and θ. Let $\mathbf{U_e}$ be the nodal generalized displacement of 14 degrees of freedom at the two ends of the composite box beam as follows:

$$\begin{aligned}\mathbf{U}^p = \langle & U_x(0), U_y(0), U_z(0), \theta(0), -U_z'(0), U_y'(0), -\theta'(0), \\ & U_x(l), U_y(l), U_z(l), \theta(l), -U_z'(l), U_y'(l), -\theta'(l)\rangle^T\end{aligned} \tag{28}$$

By substituting the coordinates at the ends of member into Eq. (27) and accounting for Eq. (28), the nodal displacement vector $\mathbf{U_e}$ can be expressed as

$$\mathbf{U_e} = \mathbf{Ha} \tag{29}$$

The displacement state vector consisting of 14 displacement components is evaluated from Eqs. (27) and (29) as follows:

$$\mathbf{d} = \mathbf{X_n H^{-1} U_e} \tag{30}$$

It should be mentioned that $\mathbf{X_n H^{-1}}$ in Eq. (30) is the exact interpolation matrix not an approximate one. For evaluation of the displacement state vector, the calculation of the coefficients by the recursive relations is continued, using a technical computing program Mathematica (Wolfram 1991), until the contribution of the next coefficient is less than an arbitrary small number.

3.2 Evaluation of dynamic stiffness matrix

The dynamic stiffness matrix of composite box beam is evaluated from the displacement state vector of the beam derived in previous section. For this purpose, we consider the force-displacement relationships in Eq. (20) of composite box beam which are expressed in a matrix form as follows:

$$\mathbf{f} = \mathbf{Sd} \tag{31}$$

where the force vector **f** are given by

$$\mathbf{f} = \langle F_1, F_2, F_3, M_1, M_2, M_3, M_\phi \rangle^T \tag{32}$$

Substituting Eq. (30) into Eq. (31), the nodal forces at the two ends of element are expressed with respect to the nodal displacements as follows:

$$\mathbf{F}^p = -\mathbf{f}(\mathbf{0}) = -\mathbf{S}\mathbf{X}_\mathbf{n}(\mathbf{0})\mathbf{H}^{-1}\mathbf{U}_\mathbf{e} \tag{33a}$$

$$\mathbf{F}^q = \quad \mathbf{f}(l) = \quad \mathbf{S}\mathbf{X}_\mathbf{n}(l)\mathbf{H}^{-1}\mathbf{U}_\mathbf{e} \tag{33b}$$

Finally, the dynamic stiffness matrix of composite box beam is evaluated based on the linear relation between the nodal displacement parameters and the member forces as follows:

$$\mathbf{F}_\mathbf{e} = \mathbf{K}\mathbf{U}_\mathbf{e} \tag{34}$$

where

$$\mathbf{K} = \begin{bmatrix} -\mathbf{S}\mathbf{X}_\mathbf{n}(\mathbf{0})\mathbf{H}^{-1} \\ \mathbf{S}\mathbf{X}_\mathbf{n}(l)\mathbf{H}^{-1} \end{bmatrix} \tag{35}$$

Here, the calculation of the dynamic stiffness matrix **K** is stopped according to a preset criteria: it could be until the relative difference of elements $|\mathbf{K_{ij}} - \mathbf{K_{ji}}|$ is less than an arbitrary small value 10^{-10}. Where a typical element in the ith row and ith column of **K** is identified as K_{ij}. The natural frequencies of vibration for the member are the values of ω that cause the dynamic stiffness matrix for the beam element to become singular as in Eq. (36). A search procedure is employed to find these values up to the desired accuracy. In this study, the Regular-Falsi method (Wendroff 1966) is applied to ensure that none of the natural frequencies is missed.

$$\det|\mathbf{K}(\omega)| = 0 \tag{36}$$

It should be noted that the dynamic stiffness matrix in Eq. (35) is formed by frequency dependent shape functions which are exact solutions of the governing differential equations. Therefore, it eliminates discretization errors and is capable of predicting an infinite number of natural frequencies by means of a finite number of coordinates.

4. FInite element formulation

For comparison, the finite element model for the composite box beam is presented. The generalized

displacements are expressed over each element as a cubic Hermintian interpolation function and substituting these displacements into Eqs. (9), (10), (13), and (16) and integrating along the element length, the total potential energy of a composite box beam are obtained in a matrix form as

$$\Pi_T = \frac{1}{2}\tilde{\mathbf{U}}_\mathbf{e}^\mathrm{T}(\mathbf{K_e}+\mathbf{K_g}-\omega^2\mathbf{M_e}+\mathbf{K_f})\tilde{\mathbf{U}}_\mathbf{e}-\tilde{\mathbf{U}}_\mathbf{e}^\mathrm{T}\tilde{\mathbf{F}}_\mathbf{e} \tag{37}$$

where $\mathbf{K_e}$ and $\mathbf{K_g}$ are the element elastic and geometric stiffness matrices, respectively, in a local coordinate. And $\mathbf{M_e}$ and $\mathbf{K_f}$ are the mass matrix and the stiffness matrix considering the foundation effect, respectively. In this study, the stiffness and mass matrices are evaluated using the Gauss numerical integration scheme and the assembly of element stiffness and mass matrices for the entire structure based on the coordinate transformation leads to the matrix equation in a global coordinate system.

5. Numerical examples

To demonstrate accuracy and validity of the present method developed by this study, the decoupled and coupled free vibration analyses of composite box beams considering the effects of the initial axial force and the elastic foundation are performed and compared with the finite element solutions using the Hermitian beam elements and the available results from other researchers.

5.1 Beams with symmetric laminations

For verification purpose, the composite box beam, as shown in Fig. 1, with symmetric laminations is considered. First, the beam is supported simply (S-S) at two ends and it is assumed that $b = 0.3$ m and $h = 0.6$ m. The length of beam is 12m and the total thicknesses of flanges and webs are 0.03m. The graphite-epoxy is used for the beam with its material properties: $E_1 = 144$ GPa, $E_2 = E_3 = 9.66$ GPa, $G_{12} = G_{13} = 4.14$ GPa, $G_{23} = 3.45$ GPa, $\nu_{12} = \nu_{13} = 0.3$, $\nu_{23} = 0.5$, $\rho = 1389$ kg/m^3. Subscripts '1' and '2' correspond to directions parallel and perpendicular to fibers, respectively. All constituent flanges and webs are assumed to be symmetrically laminated with respect to its mid-plane and the considered laminate schemes are: (a) [0/0/0/0], (b) [0/90/90/0], (c) [45/-45/-45/45].

The lowest four lateral and vertical natural frequencies obtained from the present dynamic stiffness matrix method (DSMM) are presented in Tables 1 and 2, respectively, with different stacking sequences. For comparison, the results from FE analysis using 30 Hermitian beam elements and the analytical solutions by Roberts (1987) are presented together. From Tables 1 and 2, it can be found that the solutions from this DSMM using only a single element coincide with those from FE analysis and are in an excellent agreement with those from the analytical solutions for the lamination stacking sequences under consideration. It should be noted that the present numerical solutions are exact for the higher vibrational modes as well as the lower ones because the displacement state vector in Eq. (30) satisfies the homogeneous form of the equations of motion in Eqs. (18a-d). Whereas, a large number of Hermitian beam elements are required to achieve sufficient accuracy for the higher modes due to the use of the approximate interpolation polynomials as a shape function.

Next, in Table 3, the lowest four vertical natural frequencies for S-S beams with [45/-45/-45/45] angle-ply lamination under the constant axial force by this study are given and compared with the FE

Table 1 Lateral natural frequencies (Hz) of S-S beam with different stacking sequences

Stacking sequence	Methods	Mode			
		1	2	3	4
[0/0/0/0]	DSMM	14.71	58.71	131.72	233.20
	FE analysis	14.71	58.72	131.72	233.20
	Roberts (1987)	14.71	58.86	132.43	235.42
[0/90/90/0]	DSMM	10.78	43.03	96.52	170.88
	FE analysis	10.78	43.03	96.52	170.89
	Roberts (1987)	10.78	43.13	97.04	172.51
[45/-45/-45/45]	DSMM	4.75	18.96	42.53	75.29
	FE analysis	4.75	18.96	42.53	75.29
	Roberts (1987)	4.75	19.00	42.75	76.01

Table 2 Vertical natural frequencies (Hz) of S-S beam with different stacking sequences

Stacking sequence	Methods	Mode			
		1	2	3	4
[0/0/0/0]	DSMM	24.80	98.69	220.20	387.00
	FE analysis	24.80	98.69	220.21	387.01
	Roberts (1987)	24.84	99.37	223.57	397.46
[0/90/90/0]	DSMM	18.16	72.27	161.24	283.37
	FE analysis	18.16	72.27	161.24	283.38
	Roberts (1987)	18.19	72.76	163.71	291.03
[45/-45/-45/45]	DSMM	8.01	31.86	71.10	124.95
	FE analysis	8.01	31.86	71.10	124.95
	Roberts (1987)	8.02	32.08	72.18	128.33

Table 3 Vertical natural frequencies (Hz) of [45/-45/-45/45] laminated S-S beam under the axial force, (F_{1cr} = 974967 N)

Mode	Number of Hermitian beam elements					DSMM
	5	10	15	20	30	
1	(7.2715)	(7.2707)	(7.2706)	(7.2706)	(7.2706)	(7.2706)
	8.0075	8.0067	8.0067	8.0067	8.0067	8.0067
	[8.6813]	[8.6806]	[8.6805]	[8.6805]	[8.6805]	[8.6805]
2	(31.211)	(31.161)	(31.158)	(31.158)	(31.157)	(31.157)
	31.917	31.867	31.864	31.864	31.864	31.864
	[32.607]	[32.558]	[32.556]	[32.555]	[32.555]	[32.555]
3	(70.967)	(70.437)	(70.407)	(70.401)	(70.399)	(70.399)
	71.659	71.133	71.103	71.098	71.096	71.095
	[72.344]	[71.822]	[71.792]	[71.787]	[71.785]	[71.785]
4	(127.14)	(124.47)	(124.30)	(124.27)	(124.26)	(124.26)
	127.81	125.15	124.99	124.96	124.95	124.95
	[128.48]	[125.83]	[125.67]	[125.64]	[125.63]	[125.63]

Note: ( ) natural frequency with an initial compressive force which is a half buckling load
[ ] natural frequency with an initial tensile force which is a half buckling load

solutions obtained from various numbers of Hermitian beam elements. The magnitude of the initial compressive and tensile forces applied is a half of buckling load of beam. From Table 3, it can be found that the FE solutions from at least 30 Hermitian beam elements yield the reasonably good results in the higher vibrational modes when compared with the results from DSMM using a single element.

To investigate the influence of initial axial force on the natural frequencies of composite box beams, the relative difference of the lowest four vertical frequencies for beams with various boundary conditions under the tensile force is presented in Fig. 4. The considered boundary conditions are: the clamped-free (C-F), simply- simply (S-S), clamped-simply (C-S), and clamped-clamped (C-C) boundary conditions. And ω_T denotes the frequency of beam under the tensile force. As can be seen in Fig. 4, the influence of tensile force on the natural frequencies is predominant in the first few modes. Also the effect of axial force is the highest for S-S beam, followed by C-S, C-C, and C-F beams for the 1st mode. However, for the other modes, its effect is the highest for C-C beam.

5.2 Beams with non-symmetric laminations

The non-symmetrically laminated box beam with the length $l = 0.8445$ m, the width $b = 23.438 \times 10^{-3}$m, the height $h = 12.838 \times 10^{-3}$m, and the thickness $t = 0.762 \times 10^{-3}$m is considered. The material of beam is the graphite-epoxy and its properties are as follows: $E_1 = 142$ GPa, $E_2 = E_3 = 9.8$ GPa, $G_{12} = G_{13} = 6.0$ GPa, $G_{23} = 4.83$ GPa, $\nu_{12} = \nu_{13} = 0.42$, $\nu_{23} = 0.5$, $\rho = 1445$ kg/m^3. Two particular configurations, corresponding to specific choices of lay-up have been adopted. The first one, designated circumferentially uniform stiffness (CUS), consists of a lay-up that produces the same membrane stiffness coefficients with respect to the local coordinate system. This can be described in the local coordinate system as $[\psi]_n$ along the entire circumference of the cross-section. In this case, all coupling stiffnesses are zero except

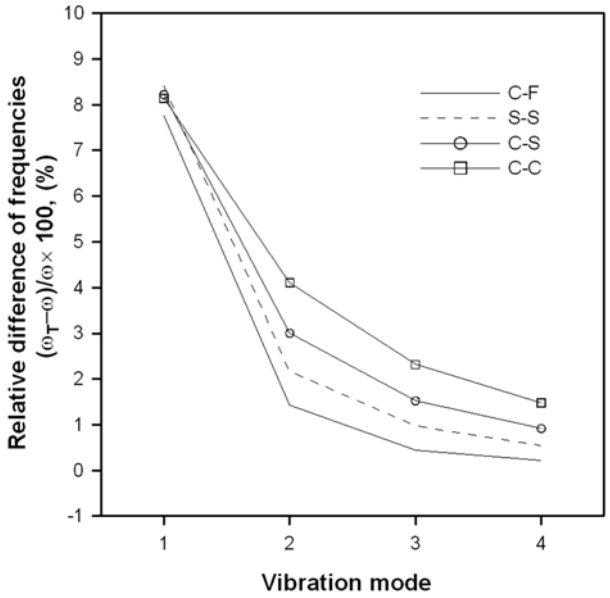

Fig. 4 Relative difference of the vertical natural frequencies for [45/-45/-45/45] laminated beams due to the tensile force

for S_ϕ. Accordingly, two flexural vibration modes are uncoupled, whereas the axial mode and the torsional one are coupled. The second lay-up is designated circumferentially antisymmetric stiffness (CAS). It is characterized by membrane shear coupling stiffness terms that are antisymmetric with respect to the local coordinate system, with all other membrane stiffness terms being symmetric. The laminate composite lay-up for this case consists of $[\psi]_n$ in the top flange, $[-\psi]_n$ in the bottom flange and $[\psi/-\psi]_{n/2}$ in the vertical webs. In this case, the coupling stiffnesses S_ϕ and H_c do not vanish. Accordingly, the lateral response is uncoupled, whereas the vertical and axial responses are coupled with the torsional one.

In Table 4, for C-F beam with CUS lay-ups, the vertical natural frequencies by the present DSMM are compared with results from FE analysis using 30 Hermitian beam elements and the several numbers of displacement based finite beam elements by Vo and Lee (2008) and the results from the extended Galerkin's method by Qin and Librescu (2002). It is seen that the frequencies by DSMM using one element are in greatly agreement with results from FE analysis and in good agreement with those from other researchers. Also for C-F beam with CAS lay-ups, the lateral frequencies are presented and compared with previously available results in Table 5. Here, Armanios and Badir (1995) used the analytical method to predict the natural frequency of composite box beam. It can be found from Table 5 that the excellent agreement between results by this DSMM and other available methods is evident.

To study the influence of compressive force on frequencies corresponding to the higher modes and on the mode shift, the variation of the 3rd flexural frequencies and the 1st axial-torsional frequency of S-S beam with CUS $[\psi]_6$ lay-up are plotted in Fig. 5 with respect to fiber angle change. The letters *Y* and *Z* in this figure refer to the frequencies corresponding to the lateral and vertical modes, respectively. Also *AT* means the axially-torsionally coupled frequency. The number in parenthesis indicates the mode number for associated vibration modes. It can be found from Fig. 5 that the flexural frequencies decrease as the fiber angle increases but the axially-torsionally coupled frequency is the maximum around $\psi = 45^o$. This is due to the fact that the stiffness components A_{66} and D_{66} in flanges and webs play an important role in torsional vibration of composite beam with closed cross-section since it affects the torsional rigidity *JG*. Thus aligning the fiber angle around 45° leads to considerable increase of the axial-torsional frequency. It is interesting to observe that the influence of compressive force on the higher flexural frequencies is not significant. While the compressive force leads to considerable reduce on the axial-torsional frequency even though this coupled mode is an enough high mode on the whole. Also the phenomenon of mode shift between the flexural mode and axial-torsional one can be observed from Fig. 5 with the change of fiber orientation. For beam without axial force, the 1st axial-torsional frequency *AT*(1), which is smaller than the 3rd flexural frequencies, becomes larger than these flexural

Table 4 Fundamental vertical natural frequencies (Hz) of C-F beam with CUS lay-ups

Stacking sequence	Vo and Lee (2008)	Qin and Librescu (2002)	This study	
			FE analysis	DSMM
$[0/30]_3$	35.53	34.58	36.71	36.71
$[0/45]_3$	32.52	32.64	33.35	33.35

Table 5 Fundamental lateral natural frequencies (Hz) of C-F beam with CAS lay-ups

Stacking sequence	Vo and Lee (2008)	Armanios and Badir (1995)	This study	
			FE analysis	DSMM
$[30]_6$	41.46	37.62	41.78	41.78
$[45]_6$	26.18	25.13	26.38	26.38

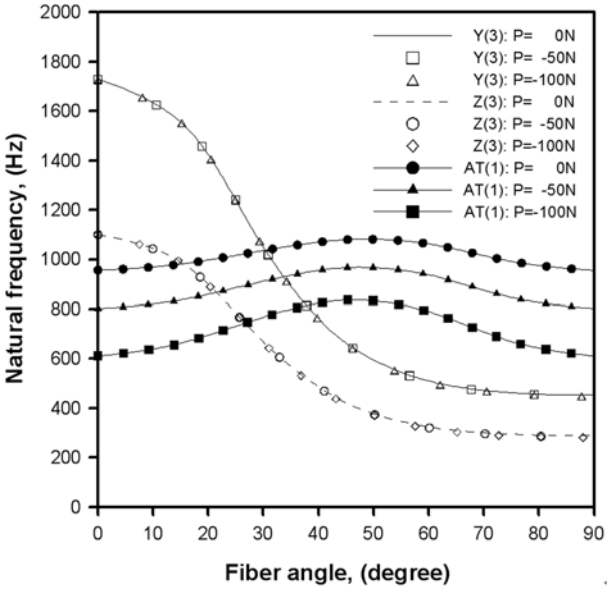

Fig. 5 Variation of the 3rd flexural frequencies $Y(3)$, $Z(3)$, and the 1st axial-torsional frequency $AT(1)$ for S-S beam with CUS $[\Psi]_6$ lay-up under the compressive force

ones through the mode shift at fiber angle $\psi = 15^o$ and $\psi = 30^o$ for the vertical and lateral modes, respectively. The value of fiber angle occurred the mode shift is increased with increase of axial force.

For C-F beam with CAS $[\psi]_6$ lay-up, the variation of the lowest three lateral and vertical-torsional frequencies is presented in Fig. 6 with respect to fiber angle change. From Fig. 6, it can be found that

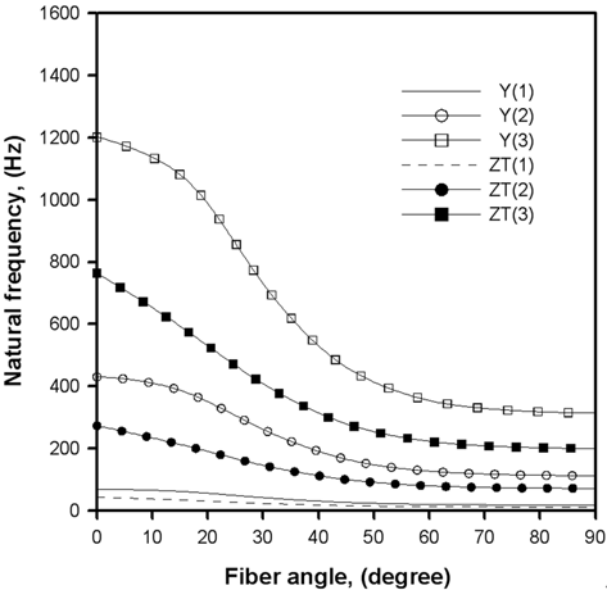

Fig. 6 Variation of the lateral and vertical-torsional frequencies for C-F beam with CAS $[\Psi]_6$ lay-up

the vertical-torsional frequencies as well as the lateral frequencies decrease as the fiber angle increases since the mode is dominated by vertical mode rather than torsional mode as shown in Fig. 7.

5.3 Beams on elastic foundation

In our final example, we consider the symmetrically laminated box beam resting on two-types of elastic foundation. The sectional and material properties used are the same as the example 5.1 and the

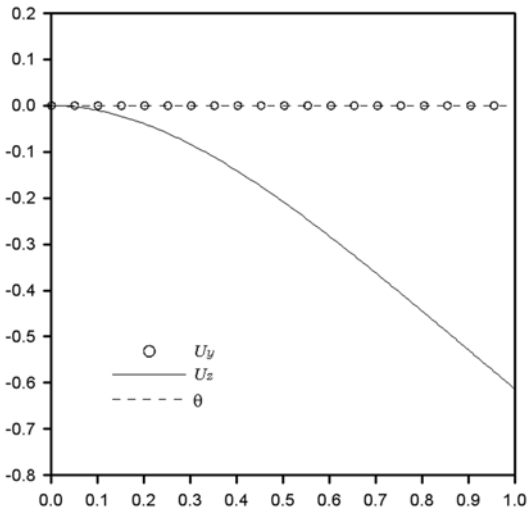

(a) CAS $[0]_6$ and CAS $[90]_6$ lay-ups

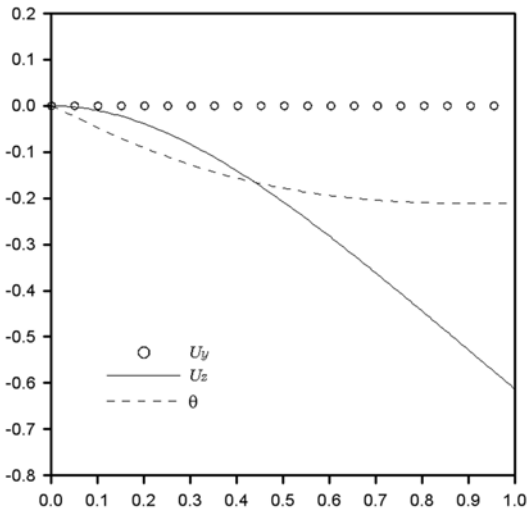

(b) CAS $[45]_6$ lay-up

Fig. 7 Mode shapes corresponding to the 1st vertical-torsional frequency *ZT*(1) of C-F beam with CAS lay-ups

foundation is modeled at the middle point of the bottom flange of the cross-section. In evaluation of the foundation parameters, the analytical method studied by Vallabhan and Das (1991) based on the modified 2-D Vlasov model is applied. This method uses experimentally determined values for the soil modulus of elasticity E_s and the Poisson ratio ν. If the soil is loose sand with $E_s = 175 \times 10^5 \text{N/m}^2$ and $\nu = 0.28$, the application of the Vallabhan-Das method produces the coefficient of sub-grade reaction $K_s = 994{,}610 \text{ N/m}^3$ and $g_z = 14{,}918{,}520\text{N}$. For a beam width $b_B = 0.3$ m and height $h_B = 0.6$ m, the Winkler foundation modulus is $k_z = K_s b_B = 298{,}383 \text{ N/m}^2$.

In Table 6, the lowest four vertical natural frequencies of the [45/-45/-45/45] laminated S-S box beam on elastic foundation by DSMM are presented and compared with the results from various numbers of Hermitian beam elements. It can be found from Table 6 that the finite element solutions from at least 30 Hermitian beam elements yield the reasonably good results in the higher vibrational modes. Fig. 8 shows the effect of foundation on the vertical frequencies of box beam for various boundary conditions. From Fig. 8, it can be found that the foundation effect decreases with increase of the vibration mode. Also contrary to Fig. 4 which shows the effect of tensile force on vertical frequency, the effect of foundation is the highest for C-F beam, followed by C-S and S-S beams. And for C-C beam, it is the lowest.

Table 6 Vertical natural frequencies (Hz) of [45/-45/-45/45] laminated S-S beam on elastic foundation

Mode	Number of Hermitian beam elements					DSMM
	5	10	15	20	30	
1	22.554 (0.99996)	22.553	22.553	22.553	22.553	22.553
2	49.807 (0.99930)	49.774	49.773	49.772	49.772	49.772
3	90.832 (0.99494)	90.402	90.378	90.373	90.372	90.372
4	147.27 (0.98268)	144.90	144.76	144.73	144.73	144.72

Note: ( ) relative frequency ratio with respect to DSMM

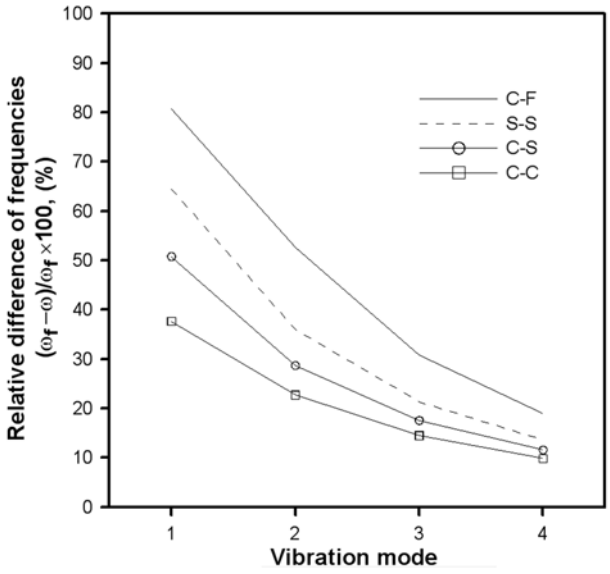

Fig. 8 Relative difference of the vertical natural frequencies for [45/-45/-45/45] laminated beams due to the foundation effects

To investigate the effect of the foundation parameters on the vertical response of box beam, for C-F beam with $[\psi/-\psi/-\psi/\psi]$lay-up, the 1st vertical natural frequency and the relative difference of this frequency due to the consideration of foundation effect are plotted in Figs. 9 and 10, respectively, with respect to the fiber angle change. These figures show that the Winkler type of foundation parameter k_z

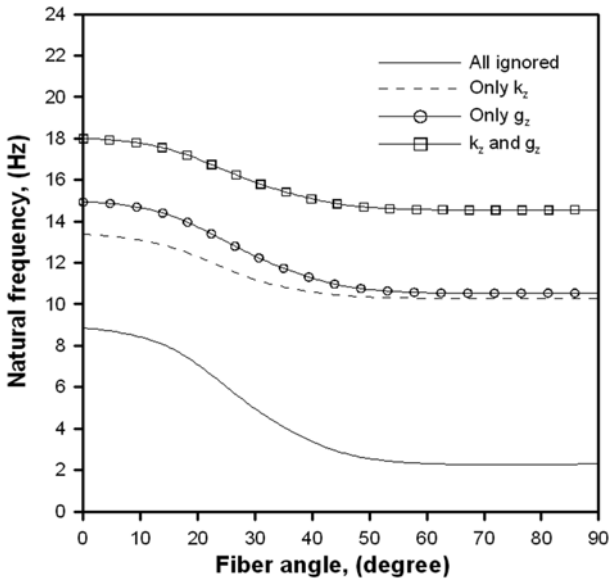

Fig. 9 Variation of the 1st vertical frequency $Z(1)$ for C-F beam on elastic foundation with $[\psi/-\psi/-\psi/\psi]$ lay-up

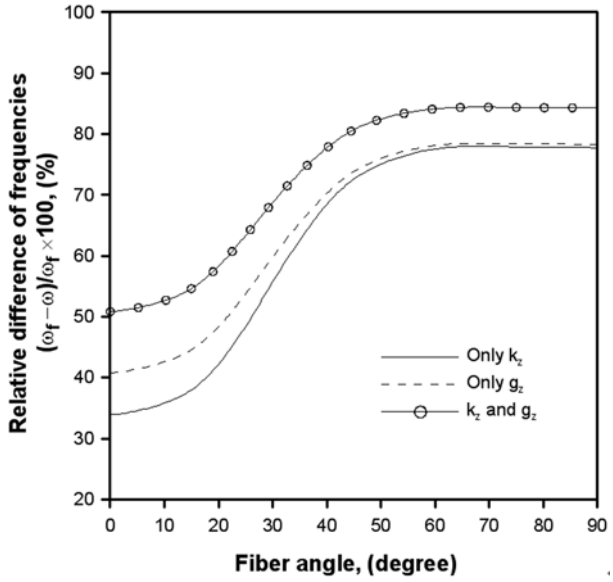

Fig. 10 Relative difference of the 1st vertical frequency $Z(1)$ for $[\psi/-\psi/-\psi/\psi]$ laminated C-F beam due to the foundation effects

and the second type of one g_z increase the flexural stiffness of the composite box beam and the effect of g_z is seen to be more larger than the effect of k_z.

6. Conclusion

The dynamic stiffness matrix is newly derived based on the power series expansion of displacement components to analyze the coupled and decoupled vibrational behavior of composite box beam resting on elastic foundation under the initial axial force. This dynamic stiffness matrix method uses the exact shape functions of the beam. Using these shape functions, the solution can be obtained with any desired accuracy yielding the exact one. An advantage, which is often overlooked but may be more important, is that the present method can provide benchmark results when compared with other results obtained by the finite element or other approximate methods. Through numerical examples, the decoupled and coupled free vibration analyses of composite box beam under the axial force with and without foundation effect are performed. The influence of the fiber orientation, the axial force, the elastic foundation, and the boundary condition on the vibrational behavior of composite box beam is parametrically investigated. The conclusions drawn from this study are as follows:

1) The natural frequencies from the present dynamic stiffness matrix method coincide with those from a large number of Hermitian beam elements and are in an excellent agreement with the analytical and finite element solutions by other researchers.

2) The influence of compressive and tensile forces on the natural frequencies is predominant in the first few modes.

3) For the CUS laminated beams, the phenomenon of mode shift between the flexural mode and axial-torsional one can be observed with the change of fiber orientation.

4) For the CUS laminated beams, the compressive force leads to considerable reduce on the axial-torsional frequency even though this coupled mode is an enough high mode on the whole.

5) For the CAS laminated beams, the vertical-torsional frequencies decrease with increase of the fiber angle since this mode is dominated by vertical mode rather than torsional mode.

6) Contrary to the effect of tensile force on vertical frequency, the effect of foundation is the highest for C-F beam, followed by C-S, S-S, and C-C beams. Also the Winkler type of foundation parameter k_z and the second type of one g_z increase the flexural stiffness of the composite box beam.

References

Abramovich, H., Eisenberger, M. and Shulepov, O. (1996), "Vibrations and buckling of cross-ply nonsymmetric laminated composite beams", *AIAA J.*, **34**, 1064-1069.

Abramovich, H., Eisenberger, M. and Shulepov, O. (1995), "Vibrations of multi-span non-symmetric composite beams", *Compos. Eng.*, **5**, 397-404.

Armanios, E.A. and Badir, A.M. (1995), "Free vibration analysis of anisotropic thin-walled closed-section beams", *AIAA J.*, **33**, 1905-1910.

Ashour, A.S. (2003), "Buckling and vibration of symmetric laminated composite plates with edges elastically restrained", *Steel Comps. Struct.*, **3**, 439-450.

Banerjee, J.R. (1998), "Free vibration of axially loaded composite Timoshenko beams using the dynamic stiffness matrix method", *Comput. Struct.*, **69**, 197-208.

Banerjee, J.R. and Williams, F.W. (1996), "Exact dynamic stiffness matrix for composite Timosheko beams with

applications", *J. Sound Vib*., **194**, 573-585.
Banerjee, J.R. and Williams, F.W. (1995), "Free vibration of composite beams-an exact method using symbolic computation", *J. Aircraft*, **32**, 636-642.
Bauld, N.R. and Tzeng, L. (1984), "A Vlasov theory for fiber-reinforced beams with thin-walled open cross sections", *Int. J. Solids Struct*., **20**, 277-297.
Chandrashekhara, K. and Bangera, K.M. (1992), "Free vibration of composite beams suing a refined shear flexible beam element", *Comput. Struct.*, **43**, 719-727.
Dancila, D.S. and Armanios, E.A. (1998), "The influence of coupling on the free vibration of anisotropic thin-walled closed-section beams", *Int. J. Solids Struct*., **35**, 3105-3119.
Dube, G.P. and Dumir, P.C. (1996), "Tapered thin open section beams on elastic foundation II: vibration analysis", *Comput. Struct*., **61**, 859-869.
Eisenberger, M. (2003a), "Dynamic stiffness vibration analysis using a higher-order beam model", *Int. J. Numer. Meth. Eng*., **57**, 1603-1614.
Eisenberger, M. (2003b), "An exact high order beam element", *Comput. Struct.*, **81**, 147-152.
Eisenberger, M. (1997), "Torsional vibrations of open and variable cross-section bars", *Thin-Wall. Struct.*, **28**, 269-278.
Eisenberger, M. (1995), "Nonuniform torsional analysis of variable and open cross-section bars", *Thin-Wall. Struct*., **21**, 93-105.
Eisenberger, M. (1994), "Vibration frequencies for beams on variable one- and two-parameter elastic foundation", *J. Sound Vib*., **176**, 577-584.
Eisenberger, M. (1990), "Exact static and dynamic stiffness matrices for general variable cross section members", *AIAA J*., **28**, 1105-1109.
Eisenberger, M. and Abramovich, H. (1997), "Shape control of non-symmetric piezolaminated composite beams", *Compos. Struct.*, **38**, 565-571.
Eisenberger, M., Abramovich, H. and Shulepov, O. (1995), "Dynamic stiffness analysis of laminated beams using a first order shear deformation theory", *Compos. Struct.*, **31**, 265-271.
Gjelsvik, A. (1981), *The theory of thin-walled bars*, Wiley, New York.
Jones, R.M. (1975), *Mechanics of composite material*, McGraw-Hell, New York.
Kisa, M. and Gurel, M.A. (2005), "Modal analysis of cracked cantilever composite beams", *Struct. Eng. Mech*., **20**, 143-160.
La, A., Singh, B.N. and Kumar, R. (2007), "Natural frequency of laminated composite plate resting on an elastic foundation with uncertain system properties", *Struct. Eng. Mech*., **27**, 199-222.
Lee, J. and Kim, S.E. (2002), "Flexural-torsional coupled vibration of thin-walled composite beams with channel sections", *Comput. Struct*., **80**, 133-144.
Lee, J. and Kim, S.E. (2000), "Free vibration of thin-walled composite beams with I-shaped cross -sections", *Compos. Struct.*, **55**, 205-215.
Marur, S.R. and Kant, T. (1996), "Free vibration analysis of fiber reinforced composite beams using higher order theories and finite element modeling", *J. Sound Vib*., **194**, 337-351.
Matsunaga, H. (2001), "Vibration and buckling of multilayered composite beams according to higher order deformation theory", *J. Sound Vib.*, **246**, 47-62.
Qin, Z. and Librescu, L. (2002), "On a shear-deformable theory of anisotropic thin-walled beams: further contribution and validations", *Compos. Struct*., **56**, 345-358.
Roberts, T.M. (1987), "Natural frequencies of thin-walled bars of open cross section", *J. Struct. Eng*., **113**, 1584-1593.
Shi, G. and Lam, K.Y. (1999), "Finite element vibration analysis of composite beams based on higher-order beam theory", *J. Sound Vib*., **219**, 707-721.
Shin, D.K., Kim, N.I. and Kim, M.Y. (2007), "Exact stiffness matrix of mono-symmetric composite I-beam with arbitrary lamination", *Compos. Struct*., **79**, 467-480.
Smith, E.C. and Chopra, I. (1991), "Formulation and evaluation of an analytical model for composite box-beams", *J. Am. Helicopter Soc*., **36**, 23-35.
Song, O. and Librescu, L. (1997), "Anisotropy and structural coupling on vibration and instability of spinning thin- walled beams", *J. Sound Vib*., **204**, 477-494.

Song, O. and Librescu, L. (1993), "Free vibration of anisotropic composite thin-walled beams of closed cross-section contour", *J. Sound Vib*., **161**, 129-147.
Song, S.J. and Waas, A.M. (1997), "Effects of shear deformation on buckling and free vibration of laminated composite beams", *Compos. Struct*., **37**, 33-43.
Vallabhan, C.V.G. and Das, Y.C. (1991), "Modified Vlasov model for beams on elastic foundations", *J. Geotech. Eng*., **117**, 956-966.
Vo, T.P. and Lee, J. (2008), "Free vibration of thin-walled composite box beams", *Compos. Struct*., **84**, 11-20.
Walker, M. (2007), "A technique for optimally designing fibre-reinforced laminated structures for minimum weight with manufacturing uncertainties accounted for", *Steel Comps. Struct*., **7**(3), 253-262.
Wendroff, B. (1966), *Theoretical numerical analysis*, Academic Press, New York.
Wolfram S. (1991), *Mathematica, a system for doing mathematics by computer,* 2nd ed., Addison-Wesley Publishing Company.
Wu, X.X. and Sun, C.T. (1990), "Vibration analysis of laminated composite thin-walled beams using finite elements", *AIAA J*., **29**, 736-742.
Yildirim, V. and Kiral, E. (2000), "Investigation of the rotary inertia and shear deformation effects on the out-of-plane bending and torsional natural frequencies of laminated beams", *Compos. Struct.*, **49**, 313-320.
Yildirim, V., Sancaktar, E. and Kiral, E. (1999), "Free vibration analysis of symmetric cross-ply laminated composite beams with the help of the transfer matrix approach", *Commun. Numer. Meth. En*., **15**, 651-660.

CC

Appendix A.

The detailed expressions of the sectional quantities in Eq. (9)

$$A = \int_C A_{11}^* ds \tag{A-1a}$$

$$S_2 = \int_C (A_{11}^* x_3 + B_{11}^* \cos\psi) ds \tag{A-1b}$$

$$S_3 = \int_C (A_{11}^* x_2 - B_{11}^* \sin\psi) ds \tag{A-1c}$$

$$S_w = \int_C (A_{11}^* \phi + B_{11}^* q) ds \tag{A-1d}$$

$$S_\phi = \int_C \left(A_{16}^* \frac{F_s}{t} - 2B_{16}^* \right) ds \tag{A-1e}$$

$$H_c = \int_C \left(-A_{16}^* \frac{F_s}{t} x_3 + 2B_{16}^* x_3 - \tilde{B}_{16}^* \frac{F_s}{t} \cos\psi + 2D_{16}^* \cos\psi \right) ds \tag{A-1f}$$

$$H_s = \int_C \left(A_{16}^* \frac{F_s}{t} x_2 - 2B_{16}^* x_2 - \tilde{B}_{16}^* \frac{F_s}{t} \sin\psi + 2D_{16}^* \sin\psi \right) ds \tag{A-1g}$$

$$H_q = \int_C \left(-A_{16}^* \frac{F_s}{t} \phi + 2B_{16}^* \phi - \tilde{B}_{16}^* \frac{F_s}{t} q + 2D_{16}^* q \right) ds \tag{A-1h}$$

$$I_2 = \int_C (A_{11}^* x_3^2 + 2B_{11}^* x_3 \cos\psi + D_{11}^* \cos^2\psi) ds \tag{A-1i}$$

$$I_3 = \int_C (A_{11}^* x_2^2 - 2B_{11}^* x_2 \sin\psi + D_{11}^* \sin^2\psi) ds \tag{A-1j}$$

$$I_{23} = \int_C \{A_{11}^* x_2 x_3 + B_{11}^* (x_2 \cos\psi - x_3 \sin\psi) - D_{11}^* \sin\psi \cos\psi\} ds \tag{A-1k}$$

$$I_\phi = \int_C (A_{11}^* \phi^2 + 2B_{11}^* q\phi + D_{11}^* q^2) ds \tag{A-1l}$$

$$I_{\phi 2} = \int_C \{A_{11}^* x_3 \phi + B_{11}^* (x_3 q + \phi \cos\psi) + D_{11}^* q \cos\psi\} ds \tag{A-1m}$$

$$I_{\phi 3} = \int_C \{A_{11}^* x_2 \phi + B_{11}^* (x_2 q - \phi \sin\psi) - D_{11}^* q \sin\psi\} ds \tag{A-1n}$$

$$JG = \int_C \left\{ A_{66}^* \left(\frac{F_s}{t} \right)^2 - 4B_{66}^* \frac{F_s}{t} + 4D_{66}^* \right\} ds \tag{A-1o}$$

Appendix B.

Equations of motion of box beam based on power series expansions of displacement components

$$\sum_{n=0}^{\infty}[A(n+2)(n+1)a_{n+2}-S_3(n+3)(n+2)(n+1)b_{n+3}-S_2(n+3)(n+2)(n+1)c_{n+3}$$
$$+S_\phi(n+2)(n+1)d_{n+2}-S_w(n+3)(n+2)(n+1)d_{n+3}-k_x a_n+\rho\omega^2 A^* a_n]x^n=0 \quad \text{(A-2)}$$

$$\sum_{n=0}^{\infty}[\tilde{I}_3(n+4)(n+3)(n+2)(n+1)b_{n+4}+\tilde{I}_{23}(n+4)(n+3)(n+2)(n+1)c_{n+4}-\tilde{H}_s(n+3)(n+2)(n+1)d_{n+3}$$
$$+\tilde{I}_{\phi 3}(n+4)(n+3)(n+2)(n+1)d_{n+4}-\frac{S_3k_x}{A}(n+1)a_{n+1}-{}^oF_1(n+2)(n+1)b_{n+2}+k_yb_n-k_y(h_z-z_p)d_n$$
$$-g_y(n+2)(n+1)b_{n+2}+g_y(h_z-z_p)(n+2)(n+1)d_{n+2}+\rho\omega^2\left\{\frac{A^*}{A}S_3(n+1)a_{n+1}-A^*b_n\right.$$
$$\left.+I_3^*(n+2)(n+1)b_{n+2}+A^*(z-z_p)d_n\right\}]x^n=0 \quad \text{(A-3)}$$

$$\sum_{n=0}^{\infty}[\tilde{I}_{23}(n+4)(n+3)(n+2)(n+1)b_{n+4}+\tilde{I}_2(n+4)(n+3)(n+2)(n+1)c_{n+4}-\tilde{H}_c(n+3)(n+2)(n+1)d_{n+3}$$
$$+\tilde{I}_{\phi 2}(n+4)(n+3)(n+2)(n+1)d_{n+4}-\frac{S_2k_x}{A}(n+1)a_{n+1}-{}^oF_1(n+2)(n+1)c_{n+2}+k_zc_n+k_z(h_y-y_p)d_n$$
$$-g_z(n+2)(n+1)c_{n+2}-g_z(h_y-y_p)(n+2)(n+1)d_{n+2}+\rho\omega^2\left\{\frac{A^*}{A}S_2(n+1)a_{n+1}-A^*b_n\right.$$
$$\left.+I_2^*(n+2)(n+1)c_{n+2}-A^*(y-y_p)d_n\right\}]x^n=0 \quad \text{(A-4)}$$

$$\sum_{n=0}^{\infty}[-S_\phi(n+2)(n+1)a_{n+2}+H_s(n+3)(n+2)(n+1)b_{n+3}-\tilde{I}_{\phi 3}(n+4)(n+3)(n+2)(n+1)b_{n+4}$$
$$-H_c(n+3)(n+2)(n+1)c_{n+3}+\tilde{I}_{\phi 2}(n+4)(n+3)(n+2)(n+2)(n+1)c_{n+4}-JG(n+2)(n+1)d_{n+2}$$
$$+\frac{S_\phi S_w}{A}(n+3)(n+2)(n+1)d_{n+3}+\tilde{I}_\phi(n+4)(n+3)(n+2)(n+1)d_{n+4}-{}^oF_1R_p^2(n+2)(n+1)d_{n+2}$$
$$-k_y(h_z-z_p)b_n+k_z(h_y-y_p)c_n+\{k_y(h_z-z_p)^2+k_z(h_y-y_p)^2+k_\theta\}d_n+g_y(h_z-z_p)(n+2)(n+1)b_{n+2}$$
$$-g_z(h_y-y_p)(n+2)(n+1)c_{n+2}-\{g_y(h_z-z_p)^2+g_z(h_y-y_p)^2\}(n+2)(n+1)d_{n+2}$$
$$\left.+\rho\omega^2\left\{\frac{A^*}{A}S_w(n+1)a_{n+1}+A^*(z-z_p)b_n-(A^*(y-y_p)c_n-I_o^*d_n+I_\phi^*(n+2)(n+1)d_{n+2})\right\}\right]x^n=0 \quad \text{(A-5)}$$